Soiling Effect in a Central Receiver Solar Plant under Real Outdoor Conditions

Alejandro Martinez[1], Iván Bravo[1], Ricardo Conceição[1,2], José González-Aguilar[1] and Manuel Romero[1]

[1] High Temperature Processes Unit, IMDEA Energy, Móstoles (Spain)

[2] Institute of Earth Sciences, Évora (Portugal)

Abstract

Reflectance loss is assessed on heliostats of the very-high concentration solar tower facility located in Móstoles, near Madrid, Spain. This region is characterized by an annual direct normal irradiance availability around 1,900 kWh/m^2, which makes it economic viable for concentrating solar power (CSP) plants. Moreover, its location nearby a highly populated area and one of the busiest highways in Spain, introduces additional features relevant in soiling analyses. The reflectance loss was measured with a Condor reflectometer on thirteen single-facet heliostats, in which nine of them are in different locations of the solar field and tilted 10º south, while four of them are side by side with different tilt angles, also turned in the same direction. The aim is to evaluate the soiling effect in an urban environment, to assess the soiling ratio and rates through the solar field, and to identify possible stow positions to reduce the soiling effect.

Keywords: Soiling, CSP, Urban Environment

1. Introduction

Particle deposition and its effect onto the optical properties in solar technologies, such as scattering and absorption (Vivar et al., 2010), have been a widely studied subject, due to its negative influence on the performance of solar power plants. Soiling decreases the transmittance and specular reflectance of surfaces, which reduces the power output of any solar energy plant. Literature in this area have been reported since the 40s of XX century (Hottel and Woertz, 1942) and have progressively evolved by introducing new techniques and developments (Pulipaka and Kumar, 2016; Sayyah et al., 2017).

Soiling effect has been widely analyzed in photovoltaics (PV) (Gostein et al., 2015; Piedra et al., 2018; You et al., 2018) stimulated by the low price of PV modules, particularly after Chinese PV production enters into the global market, and due to cheap instrumentation to measure soiling on this technology. On the other hand, soling research in concentrating solar technologies (CST) highlights a significant impact of soiling when compared with PV, because the lower acceptance angles (Bellmann et al., 2020). Current research points out that soiling can reduce the reflectance about 10% per month, even for low soiling regimes locations (Conceição et al., 2018a), and can be as high as 40% or more per month in high soiling regimes places, such as near deserts (Bouaddi et al., 2017; Merrouni et al., 2017). Moreover, besides lowering the transmittance and reflectance of glass and mirrors, it increases the operation & maintenance (O&M) costs by increases the need to clean the solar plants.

This work addresses a preliminary analysis on soiling effect in central receiver CST in an urban environment, which is extremely interesting, since reflectance related loss studies are most of the times performed near desert areas, which are characterized by high dust concentration, or in rural areas. Nevertheless, this region is located near one the largest metropoles in Spain, Madrid, and one the busiest Spanish highways, which can also be an important factor to contributing to soiling effect. For the authors' best knowledge, this study is the first ever made for the region of Móstoles, Madrid, Spain.

The paper structure is as follows: Section 2 describes the methodology used, as well as, the layout of the solar field and the selected heliostats; Section 3 includes the results for selected heliostats tilted 10º turned south, spread around the solar field, as well as, an analysis regarding four heliostats located side by side with different tilt angles;

doi:10.18086/eurosun.2020.08.01 Available at http://proceedings.ises.org

Section 4 includes an analysis regarding the soiling effect in different areas of the same heliostat; Section 5 includes a brief summary of the results and discussion.

2. Methodology

The experiment was performed at the Very-High Concentration Solar Tower (VHCST) facility (Romero et al., 2017, Martínez-Hernández et al., 2020) placed at IMDEA Energy premises in Móstoles, near Madrid. This location has a climate classified as Csa, with hot dry summers and a wet season (September to May) with rainfall events more pronounced towards the end of the year. The VHCST facility has 169 3 m^2 single-facet heliostats, see Fig. 1, that concentrate the solar radiation into a solar reactor, located at the top of the solar tower. Measurements were performed using a Condor reflectometer, developed by Abengoa Solar, on thirteen mirrors, as shown in Fig. 1. Nine heliostats were kept tilted 10º (marked by red rectangles in Fig. 1) and four were tilted 0º, 15º, 30º and 45º, respectively (marked by a green rectangle in Fig. 1), all facing south. Location of the nine heliostats was chosen to analyze the soiling variation throughout the solar field. Having four heliostats side by side, but with different slopes, allows to understand the effect of the tilt angle, which can modify soiling removal due to dew formation and rainfall events.

Each heliostat facet was measured on five different spots: top left, top right, center, bottom left and bottom right. This was performed to determine soiling distribution on the mirror surface, because soiling deposition, due to the heliostat curvature, can be higher in some areas compared to others. The measurements were performed with a Condor reflectometer, which has a resolution of ±0.001, a repeatability of ±0.002 reflectance units with 95% confidence, an accuracy of ±0.002 reflectance units [1], and the (half) acceptance aperture is 204 mrad, see Fig. 2.

Fig. 1: (Left) Scheme of the Solar field layout, with the row number marked on the left side, as well as, the heliostat number in each row, and selected heliostats to assess the soiling effect on the reflectance. Red squares indicate the heliostats that were left tilted 10º, while the green ones indicate the 0, 15, 30 and 45º tilted heliostats, from left to right, respectively; and (right) Real image, taken from the top of the Solar Tower at IMDEA Energy, Madrid, Spain.

Fig. 2: Condor reflectometer, developed by Abengoa Solar, with the VHCST on the background.

The soiling ratio, i.e., the relative reflectance loss the original clean value, was calculated as follows:

- The parameter λ is the reflectance measured with soiling, and λ_0 is the reflectance in clean state of each of the five measured locations in each mirror.
- All the measurements for each location within the same mirror, are normalized for the clean value, the maximum possible achievable reflectance, which corresponds to the $\frac{\lambda}{\lambda_0}$ term.
- Then the mean of the five ratios is calculated, which is denominated $\bar{R} = \frac{\lambda}{\lambda_0}$.
- In order to calculate the Soiling Ratio, the mean of the five ratios is subtracted to one, $1 - \bar{R}$.
- Finally, the Soiling ratio in percentage, is given by:

$$SR = (1 - \bar{R}) \times 100 \qquad \text{(eq. 1)}$$

3. Results

3.1 Fixed Tilt Positions

In Fig. 3, it is shown the soiling ratio between January 14th and March 12th. The solar field was cleaned on February 5th and February 27th, which are marked as black vertical lines in the plot. The soiling ratio throughout the solar field is always lower than 2%, which means that the selected heliostats undergo a similar behavior in terms of reflectance loss. This can be due to the small size (507 m^2) and compactness of the solar field. The SR achieves its highest value after January 20th, when a massive transport of dust from Sahara Desert reached the region of Madrid, as illustrated in Fig. 4. This will be analyzed in detail next.

Soiling rates were calculated assuming a linear function of time in those periods between heavy rainfall events when soiling tendency is to increase. These periods, named P1, P2 and P3, are identified with red dashed vertical lines in Fig. 3. The period P1 corresponds to the interval between January 20th and 23th with presence of aerosols composed of Saharan desert dust, P2 is the period between the two mirror cleanings of the solar field, and P3 comprises the period between a rain event and the latest measurements before the lockdown due to covid-19 pandemic begun.

In Table 1, the fitted soiling rates and the corresponding coefficient of determination, r^2, are given for each period, P1, P2 and P3.

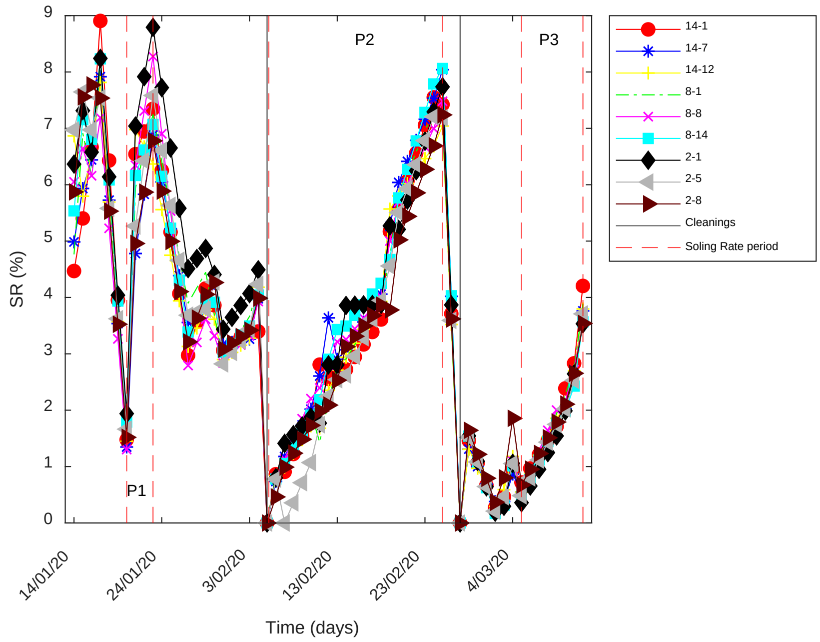

Fig. 3: Soiling ratio from January to March with the manual cleanings marked in solid grey lines and the periods (P1, P2 and P3), for which the soiling rates have been calculated.

Table 1: Soiling rates for periods with increasing soiling ratio.

Heliostat id.	***ΔSR (%)*** **(P1) | (P2) | (P3)**	***r²*** **(P1) | (P2) | (P3)**
14-1	1.80 | 0.34 | 0.45	0.71 | 0.95 | 0.89
14-7	1.77 | 0.38 | 0.41	0.90 | 0.96 | 0.92
14-12	1.45 | 0.35 | 0.41	0.51 | 0.97 | 0.93
8-1	1.79 | 0.37 | 0.42	0.79 | 0.96 | 0.95
8-8	2.19 | 0.35 | 0.40	0.83 | 0.98 | 0.96
8-14	1.63 | 0.38 | 0.39	0.74 | 0.98 | 0.94
2-1	2.14 | 0.35 | 0.42	0.81 | 0.97 | 0.95
2-5	1.90 | 0.39 | 0.41	0.91 | 0.97 | 0.93
2-8	1.67 | 0.34 | 0.37	0.88 | 0.98 | 0.94

As expected, the period P1 has the highest soiling rate, because of the fast dust accumulation and the lowest coefficient of determination compared with periods P2 and P3. The dust deposition occurred rapidly, because of the Saharan desert dust event, and did not follow a constant pace. Consequently, the soiling rate was not well-described by a linear function. In Figure 4, it is illustrated the atmospheric dust forecast provided by the Barcelona Supercomputing Center (BSC) on January 21st and 23rd. The maps point to a massive amount of dust being blown from the Sahara Desert into southern Europe, mainly Spain and Portugal. The forecasted dust load for the region of Móstoles, Madrid, is the highest possible, ≥ 4 g/m².

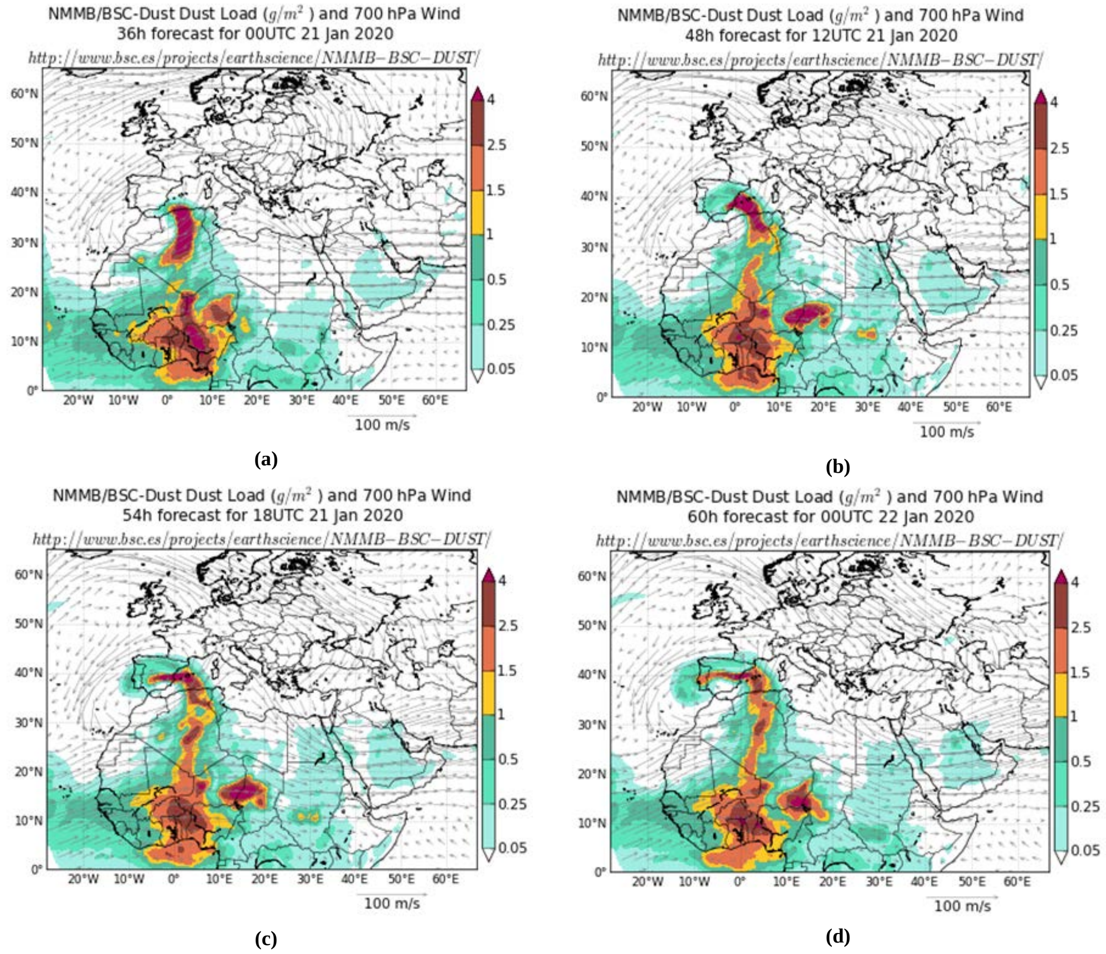

(a) (b) (c) (d)

Fig. 4: BSC dust load forecasts: a) for January 21st at 00 UTC; b) for January 21st at 12 UTC; c) for January 21st at 18 UTC; d) for January 22nd at 00 UTC.

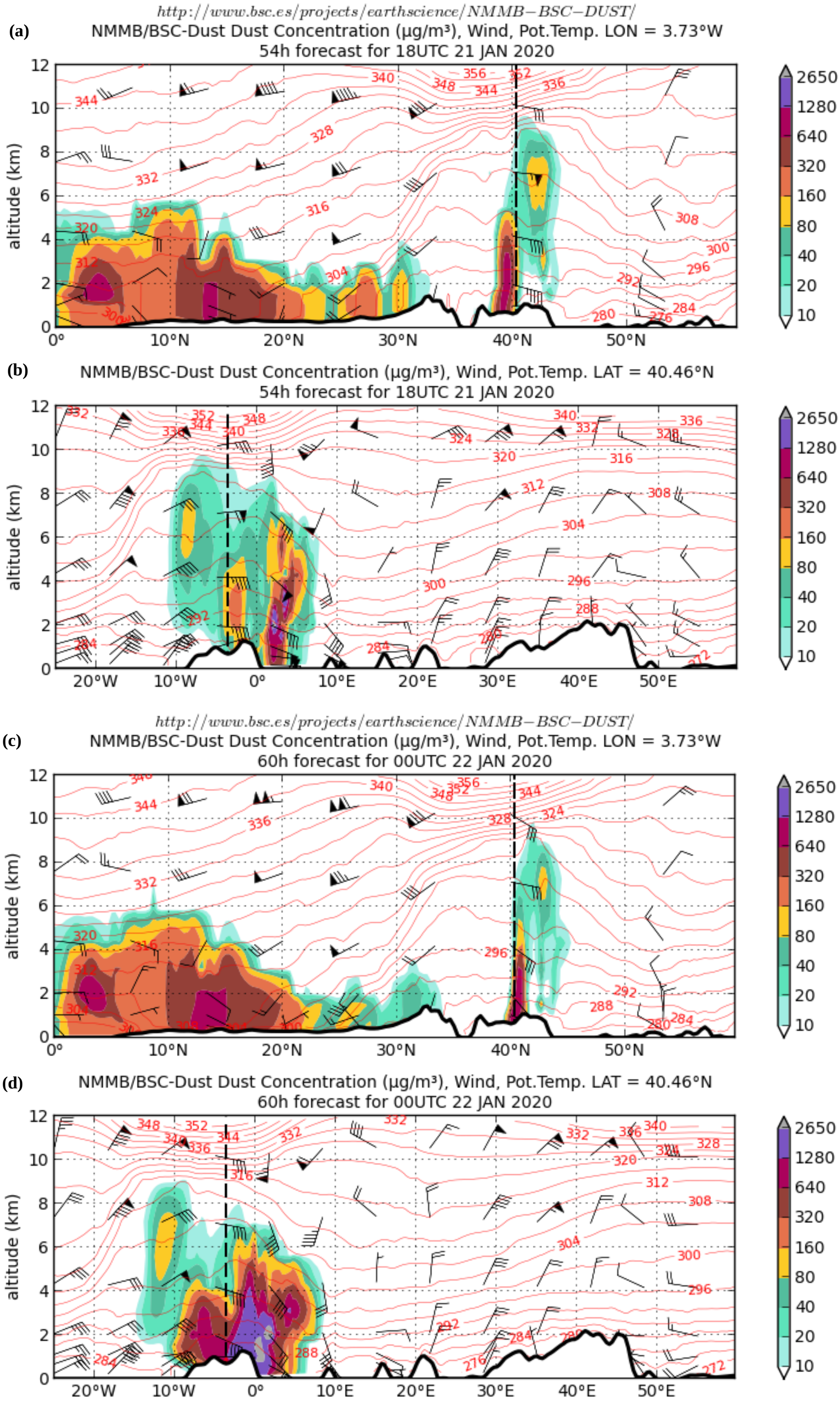

Fig. 5: BSC dust concentration forecast: (a) N-S vertical profile on January 21st; (b) W-E vertical profile on January 21st; (c) N-S vertical profile on January 22nd; and (d) W-E vertical profile on January 22nd.

Thus, based on the forecasts and on the data retrieved, it is assumed that the long-range transport of Saharan desert dust is responsible for the soiling rates between 1.45%/day to 2.19%/day for P1, the highest detected during the measurement campaign.

Moreover, on the IMDEA Energy facilities coordinates, 40.339ºN, 3.88ºW, it can be seen on Fig. 5, that the dust plume was forecasted to be suspended between 0 to 4 km, which corresponds to altitudes from where particles can easily be deposited onto surfaces on the ground. Besides this, high dust concentrations, between 640 to 2,650 μ/m^3 were forecasted for both vertical profiles.

Besides P1, from the beginning of the measurements until the solar field was first cleaned, on February 5th, this period was characterized by unstable weather conditions, with several rainfall events and possible dew formation. This also influenced soiling deposition, resuspension and removal from the heliostats, which resulted in a soiling ratio with an irregular shaped evolution.

Regarding the period P2, which basically includes all the period from the first to the second solar field cleaning, these might be the characteristic soiling rates for winter, excluding special events (such as the long-range transport of Saharan desert dust), which range between 0.34%/day to 0.39%/day. Moreover, the r^2 is close to 1.00, which indicates that the reflectance loss due to soiling during P2 is well-described by linear behavior. During this period, there was not rainfall events, which contributed to the linear increase of the soiling ratio.

The period P3, which includes the end of February and two weeks of March, also presents a soiling rate with a linear behavior, but lower correlation in comparison to P2. However, the soiling rates are higher than on P2, with values ranging from 0.37%/day to 0.47%/day. This effect is probably due to the atmospheric pollen concentration, which tends to be higher on March then on February (Subiza et al., 1995). Pollen, together with the background atmospheric particle concentration that exists every day, can increase soiling related losses (Conceição et al., 2018b). Unfortunately, due to the covid-19 lockdown, it was not possible to continue reflectance measurements during spring, but it is expected that the soiling rates can be higher than the ones obtained here, mainly on April and May.

3.2. Variable Tilted Positions

This section emphasizes the effect of the tilt angle on the reflectance loss of four mirrors selected on the same row, Fig. 6.

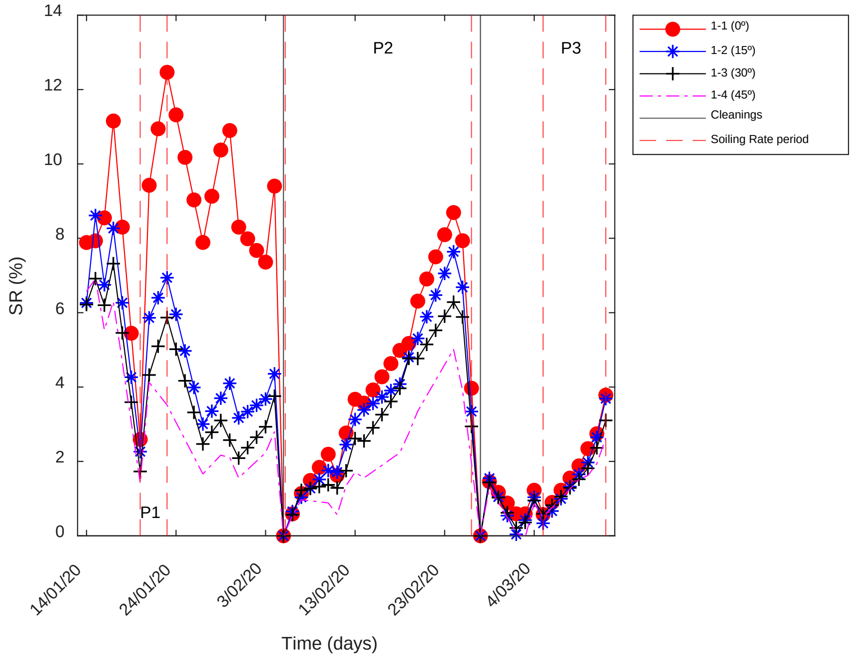

Fig. 6: Soiling ratio from January to March, for the tilt angle experiment, with the manual cleanings marked in solid grey lines and the periods (P1, P2 and P3), for which the soiling rates have been calculated.

It can be clearly seen the effect of the tilt angle when the long-range transport of Saharan desert dust happened. The horizontal heliostat reached almost 13% reflectance loss, during P1, with respect to the reference state (clean surface), whereas the 15º one reached around 6.5%. Since, according to the BSC dust forecasts, the deposition was wet, therefore it is normal to have such difference, which are about half on these two mirrors. Moreover, the higher the tilt angle, the lesser the soiling effect. It should be noted that due to the fact that deposition was in part due to light rain (that brought the dust down from the atmosphere) and because of the high tilt angle of the surface, the 45º heliostat did not get too much soiled. Instead, it got cleaned before the other mirrors, because water was able to slip from the surface, dragging particle with it.

Table 2: Soiling rates for periods with increasing soiling ratio, for the tilt angle experiment.

Heliostat id.	***ΔSR (%/day)*** **(P1) | (P2) | (P3)**	***r^2*** **(P1) | (P2) | (P3)**
1-1 (0º)	3.11 | 0.42 | 0.42	0.85 | 0.98 | 0.96
1-2 (15º)	1.46 | 0.36 | 0.44	0.79 | 0.98 | 0.94
1-3 (30º)	1.32 | 0.31 | 0.33	0.90 | 0.98 | 0.94
1-4 (45º)	0.60 | 0.22 | 0.27	0.40| 0.90 | 0.96

Moreover, it can be seen in Table 2 that during P2, both the 1-1 (0º) and the 1-2 (15º) have soiling rates similar to heliostats shown in Table 1. This is because the ones in Table 1 were tilted 10º. The significant differences appear on the 1-3 (30º) and 1-4 (45º) heliostats. Namely the heliostat with less soiling, regardless of the period, is the one tilted 45º, with extremely low soiling rates, around 0.22%/day to 0.27%/day. This is indeed the position less prone to soiling, and highest probability to be efficiently cleaned by rainfall, and it should be used for the resting position for the solar field. This probably can reduce the reflectance loss during winter and avoid some cleanings, therefore spending less capital during this season. Moreover, during this season, there were not many rainfall events, and one can assume that, if it rains more frequently during this period, and if the 45º position is used, it might be possible to not clean the solar field from January to March, and still maintain a reflectance loss under 10% , which should be enough for any experiments to be performed at the solar tower without any problem.

3.3. Intra-mirror Variation

It is important to understand how the mirror tilt is correlated with the soiling deposition, within different areas within the same mirror. For that, the data corresponding to the four heliostats tilted is used and compared. The mean of the standard deviation of the five measured positions for each heliostat, for the entire measuring campaign, was calculated and it is shown on Fig. 7.

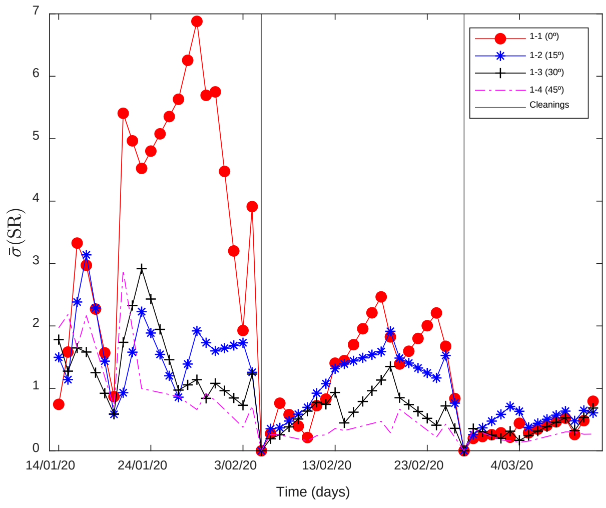

Fig. 7: Mean of the standard deviation for the five positions measure in each of the four tilted heliostats.

As it can be seen, the highest standard deviations are seen for the horizontal heliostat (0º), and the trend detected is that the soiling deposits (or is washed) in a more homogenous way, with higher tilt angles. Moreover, data analysis, not shown here, demonstrates that the most critical soiling areas within the mirror are the center and the bottom part. The center accumulation is and due to low tilt angles, because water from rainfall will accumulate there until it dries, leaving a pool of dust, see Fig. 8, and because the fact that the surface is curved. The bottom particle accumulation, is due to the fact that the tilt angle may not be enough for water to completely slip away from the heliostats' surface. This creates a small water layer at the bottom edge of the heliostats' surface, and when it dries, it leaves that area of the heliostat soiled. It should be noted that sometimes the accumulation will not be at the center of the heliostat, but will be a little moved, due to the fact that the surface is not perfectly curved and the heliostat is not perfectly tilted south.

Fig. 8: Soiling accumulation near the center part of a heliostat due to low tilt angle resting position, and soiling accumulation on the bottom part of the surface.

This means that higher tilt angles are important not only to reduce soiling effect, as seen in the previous sections, which is a direct consequence of less particle deposition at such high slopes, and the fact that is easier from rainfall to clean the surface, but it is also important to maintain a higher degree of soiling deposition homogeneity. This homogeneity can be advantageous: from a cleaning point of view, it can probably be easier to clean and do it faster on a surface that does not have localized and hard bounded soiling in multiple layers; from an optical point of view, it might be the case that non-homogenous soiling deposition, for instance in the center of the heliostat, and considering that its surface is not perfectly curved, can reduce and modify the flux map at the target, resulting in a lower performance.

4. Conclusions

A soiling campaign was recorded from January to March 2020 on the heliostats of the VHCST located at IMDEA Energy in Mostoles, Madrid, Spain. Regarding soiling assessment, 9 heliostats, tilted 10º, were used. It was seen that the soiling effect is similar for different positions of the solar field, which can be due to the fact that the area occupied by the solar field is small. It was also detected that for this part of the year, from January to March, that soiling effect can reduce reflectance around 10% or more, depending on the tilt angle. More specifically it was seen that during January, the soiling ratio reached its highest value, which was due to a long-range transport of Saharan desert dust. During February, due to the lack of rainfall events, the soiling ratio behaved in a linear fashion, which is in line with results obtained in other studies. The soiling rate, which already include part of March, shows higher values than the one of February, which can be due to the higher atmospheric pollen concentration.

Therefore, it is concluded, from the measured data, that soiling can be a problem in this region, because the high soiling rates, even though it is not located near a desert, especially considering the season. Moreover, long-range transport of Saharan desert dust can reach this location, which can increase very rapidly the reflectance loss.

Future work will imply a longer solar campaign, including the dry season, to characterize what type of soiling deposits in the location, to characterize seasonal and annual trends of the soiling effect, to compare soiling rates between different seasons, and to study possible cleaning scenarios and schedules.

5. Acknowledgments

The data and/or images from the (NMMB/BSC-Dust or BSC-DREAM8b) model, operated by the Barcelona Supercomputing Center (http://www.bsc.es/ess/bsc-dust-daily-forecast/) is acknowledge. This project has received funding from the European Union's Horizon 2020 research and innovation programme under grant agreement Nº 823802 (SFERA III). The authors wish to thank to “Comunidad de Madrid” and European Structural Funds for their financial support to ACES2030-CM project (S2018/EMT-4319). AMH also acknowledge support from the Community of Madrid (Spain) through the Young Employment Program (PEJD-2017-PRE/AMB-4951).

6. References

Bellmann, P., Silva, H.G., Wolfertstetter, F., Conceicao, R., 2020. Comparative modelling of optical soiling losses for CSP and PV devices in regard to gravimetric density. Sol. Energy 197, 229–237.

Bouaddi, S., Ihlal, A., Fernández-García, A., 2017. Comparative analysis of soiling of CSP mirror materials in arid zones. Renew. Energy 101, 437–449. https://doi.org/10.1016/j.renene.2016.08.067

Conceição, R., Silva, H.G., Collares-Pereira, M., 2018a. CSP mirror soiling characterization and modeling. Sol. Energy Mater. Sol. Cells 185. https://doi.org/10.1016/j.solmat.2018.05.035

Conceição, R., Silva, H.G., Mirão, J., Collares-Pereira, M., 2018b. Organic Soiling : The Role of Pollen in PV Module Performance Degradation. Energies Special Ed, 1–13. https://doi.org/10.3390/en11020294

Gostein, M., Duster, T., Thuman, C., 2015. Accurately measuring PV soiling losses with soiling station employing module power measurements. 2015 IEEE 42nd Photovolt. Spec. Conf. PVSC 2015 3–7. https://doi.org/10.1109/PVSC.2015.7355993

Martínez-Hernández, A., Gonzalo, I.B., Romero, M., González-Aguilar, J., 2020. Drift analysis in tilt-roll heliostats. Solar Energy 211, 1170-1183. https://doi.org/10.1016/j.solener.2020.10.057

Merrouni, A.A., Mezrhab, A., Ghennioui, A., Naimi, Z., 2017. Measurement, comparison and monitoring of solar mirror’s specular reflectivity using two different Reflectometers. Energy Procedia 119, 433–445. https://doi.org/10.1016/j.egypro.2017.07.045

Piedra, P.G., Llanza, L.R., Moosmüller, H., 2018. Optical losses of photovoltaic modules due to mineral dust deposition: Experimental measurements and theoretical modeling. Sol. Energy 164, 160–173. https://doi.org/10.1016/j.solener.2018.02.030

Pulipaka, S., Kumar, R., 2016. Power prediction of soiled PV module with neural networks using hybrid data clustering and division techniques. Sol. Energy 133, 485–500. https://doi.org/10.1016/j.solener.2016.04.004

Romero, M., González-Aguilar, J., Luque, S., 2017. Ultra-modular 500m2 heliostat field for high flux/high temperature solar-driven processes. AIP Conf. Proc. 1850. https://doi.org/10.1063/1.4984387

Sayyah, A., Eriksen, R.S., Horenstein, M.N., Mazumder, M.K., 2017. Performance Analysis of Electrodynamic Screens Based on Residual Particle Size Distribution. IEEE J. Photovoltaics 7, 221–229. https://doi.org/10.1109/JPHOTOV.2016.2617088

Vivar, M., Herrero, R., Antón, I., Martínez-Moreno, F., Moretón, R., Sala, G., Blakers, A.W., Smeltink, J., 2010. Effect of soiling in CPV systems. Sol. Energy 84, 1327–1335. https://doi.org/10.1016/j.solener.2010.03.031

You, S., Lim, Y.J., Dai, Y., Wang, C.H., 2018. On the temporal modelling of solar photovoltaic soiling: Energy and economic impacts in seven cities. Appl. Energy 228, 1136–1146. https://doi.org/10.1016/j.apenergy.2018.07.020